La Metallurgia Italiana
International Journal of the Italian Association for Metallurgy

DOI 10.36146/2026_06_09

Optimization of Electric Arc Furnace refining via CFD simulation of steel, slag, and freeboard dynamics

O. Ugarte, S. Aryal, T. Okosun, E. Pretorius, J. Maiolo, C. Kovscek, C. Q. Zhou

This study presents a state-of-the-art CFD methodology to simulate the industrial EAF refining stage. The model incorporates jet-induced cavities within a volume-of-fluid representation of the molten steel, slag, and freeboard regions, capturing oxygen-steel reactions, decarburization, oxide formation, and oxide migration from metal to slag and freeboard. Validation against theoretical predictions demonstrates accurate modeling of decarburization and FeO/MnO generation across both high and low carbon regimes. The model is then applied to evaluate reduced oxygen injection scenarios by turning off oxygen jets at 200 sec and 400 sec. Results show that lowering the O_2 injection rate could decrease decarburization performance by ~5% while reducing FeO formation by up to 53%. This FeO reduction lowers carbon-injection requirements for slag foaming, offering potential decreases in operating cost and CO_2 emissions in EAF operations.

KEYWORDS: ELECTRIC ARC FURNACE; SLAG; MOLTEN STEEL; REFINING; VOF; CFD.

INTRODUCTION

In recent years, the steel industry has shifted from the blast furnace-basic oxygen furnace (BF-BOF) route to Electric Arc Furnace (EAF) steelmaking. In the United States, more than 70% of steel production now occurs in EAFs. EAF operations offer improved energy efficiency and operational flexibility and can reduce carbon emissions by up to 55% compared with BF-BOF [1]. The EAF process consists of melting and refining operations. During melting, electrodes and burners supply arc and chemical heat to melt the scrap charge. During refining, burners switch to lance mode, and oxygen is injected into the molten bath to remove carbon, form oxides, and eliminate impurities to reach the desired steel chemistry and temperature before tapping.

EAF refining involves multiple physicochemical processes, making process understanding and optimization challenging. Oxygen-bath interaction, in particular, plays a key role in controlling oxidation reactions which are critical for steel uniformity and quality, and extensive research has been devoted to understanding this process. For instance, Banks and Chandrasekhara [2] performed experiments on gas injection into liquid at right angles and showed that cavity penetration depth decreases

Orlando Ugarte, Shishir Aryal, Tyamo Okosun, Chenn Q. Zhou
Center for Innovation through Visualization and Simulation (CIVS) & Steel Manufacturing Simulation and Visualization Consortium (SMSVC) Purdue University Northwest; Hammond, IN, U.S.A

Eugene Pretorius
Nucor Steel Berkeley; Huger, SC, U.S.A

Joe Maiolo
Linde Inc., Tonawanda, NY, U.S.A

Chris Kovscek
Nucor Steel; Jewett, TX, U.S.A

when the liquid is in motion. Alam et al. [3] studied lance angle, lance height, and flow rate effects on wall splashing and found that splashing increases with these parameters up to a critical point, after which it decreases. This study recommended low lance heights and coherent jet nozzles to reduce splashing.

The introduction of coherent jets in the 1990s, which inject oxygen at supersonic speeds, significantly improved EAF productivity by maintaining jet momentum, enhancing bath stirring, and accelerating refining reactions [4]. Oxygen injection also drives iron oxide formation, which is essential for slag formation and slag foaming. Slag foaming insulates the arc, reduces heat losses, and increases productivity. However, excessive FeO leads to yield losses and deteriorates slag foaming behavior. Carbon injections are therefore required to control FeO content and recover iron, motivating extensive research into optimizing practices involving them. Strelbisky et al. [5] implemented Tallman supersonic carbon injectors, achieving substantial reductions in carbon consumption and CO_2 emissions. Linde has also developed a three-in-one supersonic injector that integrates oxygen lancing, carbon injection, and oxy-fuel combustion to reduce carbon losses and improve efficiency of carbon delivery [6].
Research on oxygen injections, cavity formation, and carbon injections has been strongly linked to refining performance. Several models have been developed to optimize refining operations. Memoli et al. [7] created a theoretical model to predict jet penetration and decarburization under various operating conditions. Wei and Zhu [8] developed a thermodynamic model showing how competition among C, Cr, Si, and Mn for oxygen evolves during refining in the AOD process; they identified a critical carbon concentration range (0.25-0.4% C) where decarburization becomes mass-transfer-controlled.

Prior research at the Center for Innovation through Visualization and Simulation (CIVS) at Purdue University Northwest developed advanced CFD models for industrial EAF refining operations. Chen et al. [9-11] introduced an integrated method dividing the refining process into three sequential calculations: supersonic coherent jet, cavity formation in bath due to jet impingement, and stirring and reactions in refining simulations, avoiding the need to directly model high-speed oxygen injection in EAF refining. Moreover, the effect of oxygen flow rate on bath mixing [12] and the trade-offs between oxygen flow rate, decarburization performance, and FeO-related yield losses [13] were also studied. However, these studies did not account for the direct interaction between the metal and slag phases. In particular, the previous approach considered only the molten bath and the injected gas, while oxides were removed through the top boundary to mimic the effect of the slag layer. The present study introduces a CFD framework that explicitly incorporates metal-slag interactions during refining operations. This is achieved by applying the Volume of Fluid (VOF) methodology to capture the metal, slag, and gas phases simultaneously. Unlike the previous approach, this methodology does not impose limitations on phase interactions, allowing phenomena such as mixing, stirring, oxide formation, and oxide transport to the slag and freeboard regions to be directly resolved. The model is applied to an industrial EAF operation provided by Nucor Jewett and validated against theoretical predictions. The validated model is then used to investigate the impact of reduced oxygen flow rates on refining performance.

METHODOLOGY

Based on a previous approach [9], the oxygen injection produced at supersonic velocities is separated from the refining simulation by applying a three-step process. First, coherent-jets simulations are performed to determine the jet velocity and composition of injected oxygen when it reaches the bath surface. Second, the results provided by coherent-jet simulations are used to determine the cavities forming in the surface of the bath as a result of oxygen injection. Third, the computed cavities are added to a refining CFD domain where oxygen injected at the cavities interact with molten steel to generate oxides. The refining simulation includes the molten steel, slag and freeboard and oxidation reactions of Fe, C and Mn. Figure 1 shows these steps. Further details, including mathematical formulation, are included in Ref [9, 12-13].

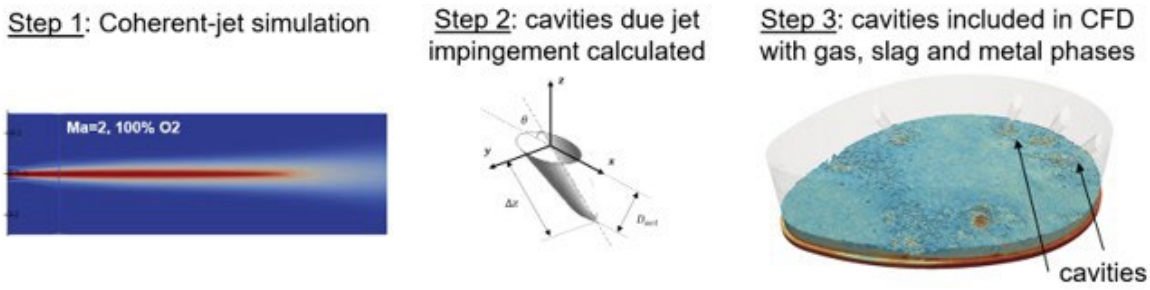

Fig.1 - Three steps methodology used in CFD simulations of EAF refining process.

Computational domain:

As mentioned earlier, steps 1 and 2 provide the cavities forming in the surface of the molten bath due to supersonic oxygen injection. These cavities are included in the CFD domain of the refining simulation (step 3 in figure 1). Figure 2a shows the computational domain of the EAF refining simulation. The cavities are pre-calculated based on four coherent-jets injecting oxygen at 1000 SCFM. The domain geometry and operation parameters were provided by Nucor Jewett. The CFD domain has 0.9 million non-structured cells, where solid surfaces are assumed to be adiabatic walls. Figure 2b shows key dimensions, and the location of the 4 cavities formed by the coherent-jets are shown in figure 2c.

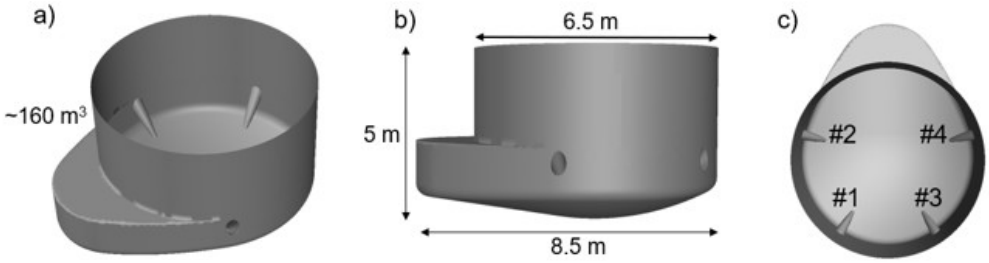

Fig.2 - Computational domain used in refining simulations including location of cavities due to oxygen injection.

VALIDATION

The CFD refining model is validated against theoretical predictions [14]. Namely, a typical operation is simulated in Nucor Texas (NSTX) EAF without injection of carbon particles and compared with decarburization and FeO production predicted by theory. Table 1 lists key parameters applied in the validation case.

Tab.1 - Parameters used in the validation (baseline) simulation.

BASELINE OPERATION PARAMETERS	
Variable	**Value**
Number of coherent jets	4
O_2 rates in each jet [SCFM]	1000
Steel liquid temperature	1850 K (1576 °C)
C initial content in steel [%]	0.41%
Mn initial content in steel [%]	0.25%
Molten steel mass	144 tons
Initial slag mass	28 tons

Results of the validation are shown in figure 3. The CFD results accurately predict the decar-burization process (figure 3a), capturing the rapid carbon removal from the molten steel during the first two minutes. Once the dissolved carbon reaches 0.3%, decarburization becomes controlled by carbon transport within the bath rather than by gas avail-

ability. At low carbon levels, the rate slows as carbon must diffuse to the O_2 injection sites, leading to the reduced decarbu-rization rate observed after two to three minutes. Figure 3b shows the FeO increase in the slag. Although the initial FeO rise is overpredicted, the model aligns with theoretical trends as lower carbon content allows more FeO to form. It should be noted that the CFD results are compared against theoretical predictions that do not account for carbon injection. In industrial EAF operations, carbon injection is commonly employed to control FeO levels, promote slag foaming, and minimize metallic yield losses. Furthermore, the formation of other oxide spe-cies, including CaO, Al_2O_3, MgO, and SiO_2, is not considered in the set of chemical reactions included in the present CFD model.

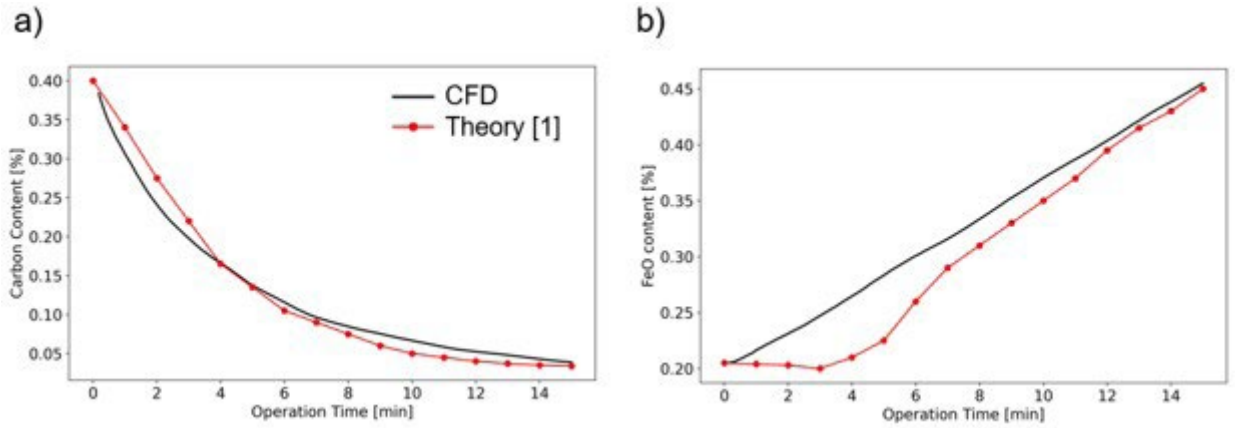

Fig.3 - CFD prediction of decarburization and FeO content compared with theoretical prediction reported in Ref [14].

RESULTS AND DISCUSSION

Decarburization and FeO production in baseline simulation

CFD results for the baseline case show clear spatial and temporal variations during the refining operation (figure 4). In the first two minutes, carbon content decreases rapidly (figure 4a-b), while changes slow significantly afterward, particularly during the final five minutes of the 15-minute refining period (Figure 4c-d). The opposite trend appears in FeO production. Initially, the FeO production rate is low (figure 4e-f), but it significantly increases as the decarburization rate declines and oxygen reacts primarily with Fe in the molten steel (figure 4g-h). Figure 4 also shows that reactions do not occur uniformly throughout the bath, but they are driven by oxygen injections forming cavities near the furnace walls.

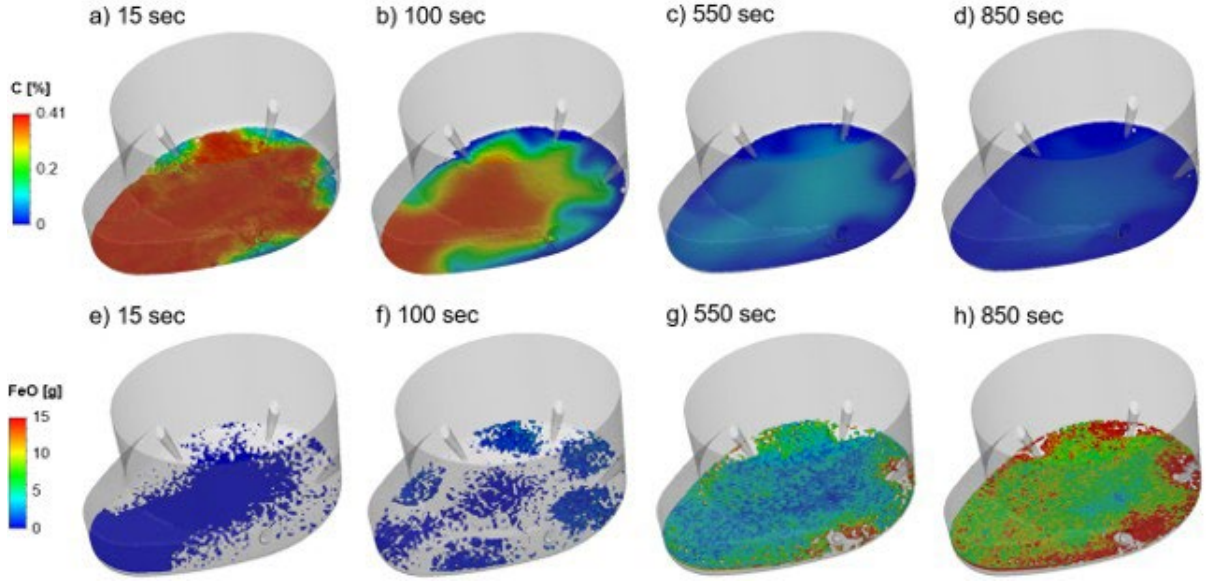

Fig.4 - Simulation results of decarburization and FeO production in actual EAF refining operation.

Decarburization and FeO production in baseline simulation

The spatial and temporal variations of oxidation reactions in figure 4 demonstrate that refining can be optimized by dynamically adjusting oxygen injections during the process. For instance, oxygen injections can be reduced after 2-3 minutes since oxidation reactions mostly lead to FeO after this period. However, the reduction of oxygen injections can also lead to poor bath stirring which affects the refining performance. Figure 5 compares the baseline case with two cases where oxygen injection is reduced by turning jets off during the operation. The first reduced oxygen case turns jets 1 and 3 off at 200 sec, and the second case turns jets 1 and 3 off at 400 sec (see figure 2c for jet locations). Figure 5 compares the carbon and FeO fields at 600 sec for the three cases. Figures 5a-c show how carbon content increases as less oxygen is injected. The larger difference is seen in figure 5b where oxygen rate is reduced at earlier time. The corresponding FeO production results are shown in figures 5d-f. Here, both cases with reduced oxygen injection show significant reduction of FeO content as compared with baseline cases.

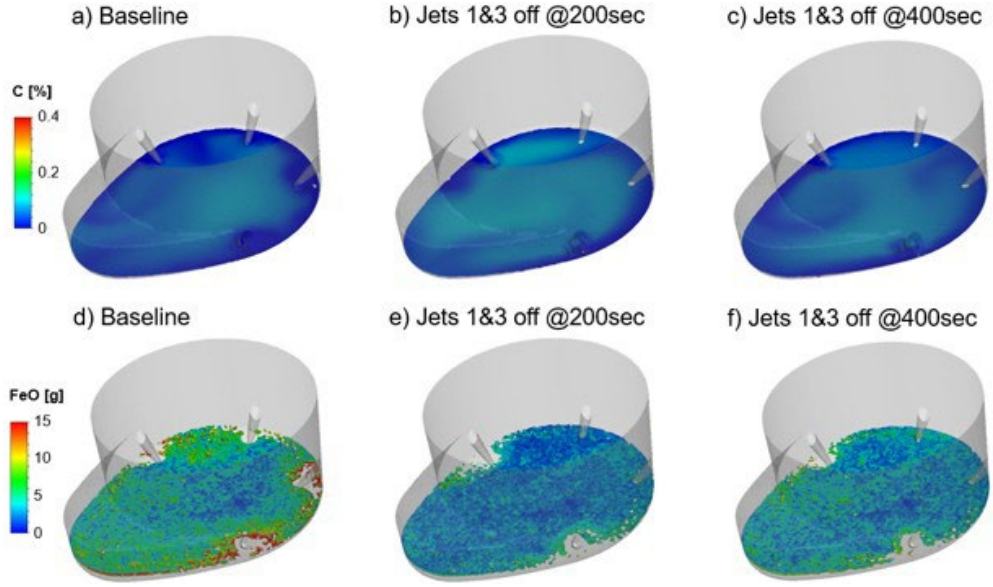

Fig.5 - Comparison of baseline and cases with reduced oxygen injection at 600 sec.

Figure 6 shows the carbon and FeO trends along the refining operation for the three cases compared in figure 5. The reduced oxygen scenarios are shown in orange lines, where solid line indicates jets turned off at 200 sec and dashed line shows the case with jets turned off at 400 sec. The larger impact of reducing oxygen is seen in the FeO production. This is expected as decarburization at later stage is significantly less efficient as concluded from figures 4a-d.

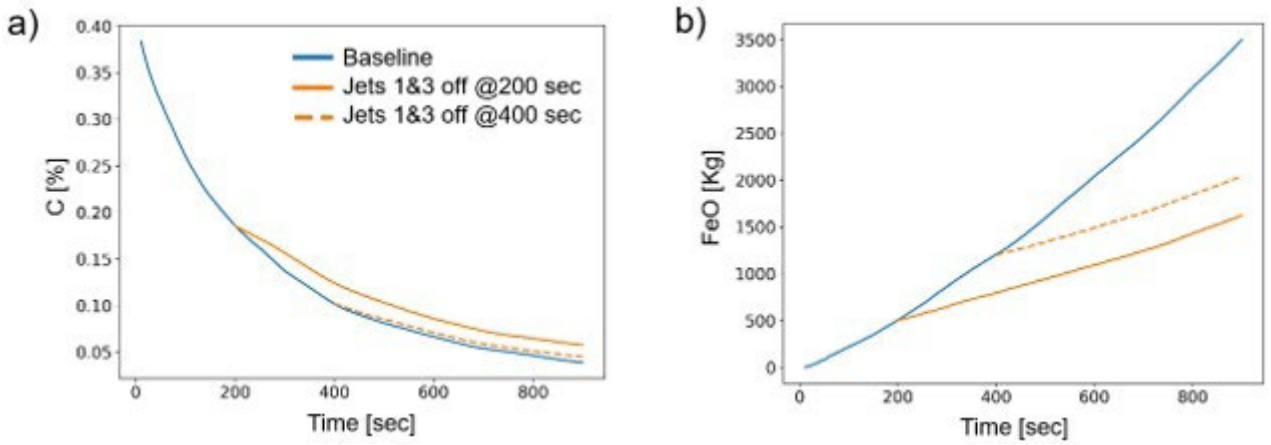

Fig.6 - Carbon and FeO trends along refining operation for baseline case (blue), case with jets 1 & 3 off at 200 sec (orange-solid) and case with jets 1 & 3 off at 400 sec (orange- dashed).

Table 2 quantifies the impact of lowering oxygen injection. Specifically, turning off two of the four oxygen jets at 200 sec reduces decarburization by 5.5% relative to the baseline case. Also, the reduction of oxygen injection at 200 sec lowers FeO production by 53.6%. If the changes are applied later at 400 sec, the impact on decarburization is 2.1%, and FeO still shows a large impact as it is reduced by 41.5% relative to the baseline case.

Tab.2 - Variation in decarburization and FeO production due to lowered oxygen injection.

IMPACT OF O_2 RATE ON REFINING REACTIONS			
Cases	**O_2 rate [SCFM]**	**Decarburization after 900 sec**	**FeO generation [kg] after 900 sec**
Baseline	4000	89.3 %	3496.1 kg
Jet #1 & #3 off at 200 sec	2000	83.8 (-5.5%)	1621.5 (-53.6%)
Jet #1 & #3 off at 400 sec	2000	87.2 (-2.1%)	2044.5 (-41.5%)

Variations in decarburization and FeO production have an impact on slag foaming as well. Slag foaming is driven by bubbles produced mostly due to carbon reactions in the molten bath and by suspended particles. It benefits EAF process as the foamed slag shrouds the electric arc and prevent thermal losses. Slag height is computed based on procedure shown in Ref [15]. The slag viscosity used in this formulation has been modified to include the impact of suspended particles by using the formulation of Krieger and Dougherty [16]. Figure 7 shows the slag height for the baseline (figure 7a) and the case with two jets turned off at 200 sec (figure 7b). Carbon injection is considered in these calculations as it is required to sustain slag foaming by boosting carbon reactions while preventing excessive FeO in slag. Carbon injection efficiency is considered by including 70% and 90% efficiency cases, which determines how much injected carbon is actually used in slag reactions. Results show that slag height increases rapidly in the beginning due to high decarburization at early stage. As the refining process progresses, CO bubbles in slag escape and slag foaming is lowered. In the baseline, 715 kg of carbon particles are injected, and the slag height is maintained above 0.5 m for the 90% carbon injection efficiency (figure 7a). For the case with reduced oxygen injection (figure 7b), 455 kg of carbon injection is needed to obtain similar slag height, reducing the additional carbon injection by 36%. The reduction of injected carbon reduces operation costs but also reduces the carbon emissions in EAF operations, as carbon injections can account for ~40% of EAF emissions [17]. Therefore, reducing the oxygen injection rate during refining may offer opportunities for process optimization. However, it should be noted that oxygen injections also play a critical role in promoting bath stirring and, consequently, temperature homogenization within the molten steel. This effect is particularly important in AC furnaces, where electromagnetic stirring is less significant than in DC furnaces. Changes in oxygen injection rates can alter the thermal distribution within the molten bath because the heat released by oxidation reactions is transported through the bath by fluid motion. As a result, reduced stirring may lead to larger local temperature gradients, which can affect refining efficiency and final product quality. Therefore, thermal homogenization should be considered alongside refining performance when determining optimal oxygen injection practices.

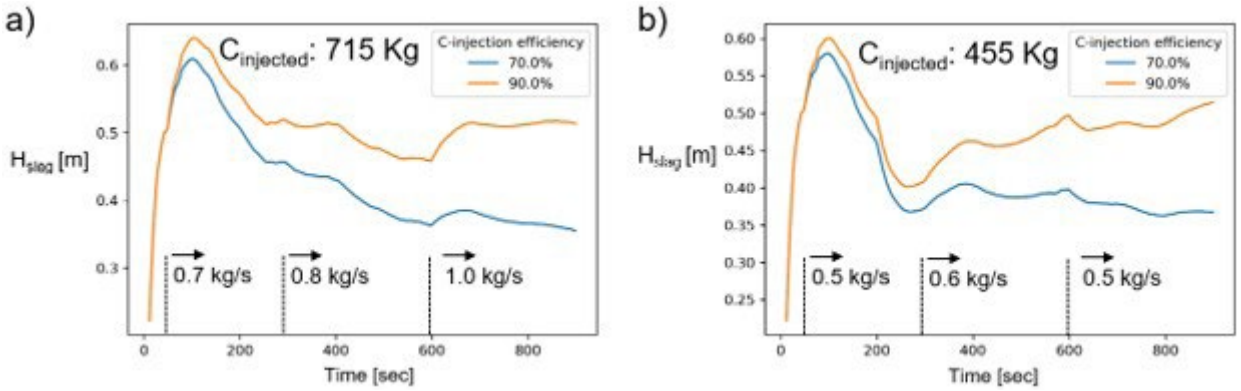

Fig.7 - Slag height for baseline case and case with jets 1 & 3 off at 200 sec, including carbon injection. Two carbon efficiencies are considered for each case, 70% and 90%.

CONCLUSIONS

In this study, a CFD framework is applied to analyze refining operations in an industrial Electric Arc Furnace (EAF) provided by Nucor Jewett. The model extends previous work by explicitly incorporating the slag and freeboard regions in addition to the molten steel phase and the chemical reactions considered in earlier studies. This enhanced approach enables the direct resolution of key refining mechanisms, including bath stirring, phase mixing, and their influence on oxidation reaction rates. The framework employs a Volume of Fluid (VOF) methodology to capture the gas, slag, and molten steel phases, model the oxidation of carbon, iron, and manganese within the molten steel, and track the transport of the resulting oxides into the slag and freeboard regions.

A baseline case was modeled in which four coherent jets supply oxygen at 1000 SCFM each. The injected oxygen interacts with 144 tons of molten steel containing 0.41% C and 0.25% Mn, along with 28 tons of slag, over a 15-minute refining period. CFD results were validated against theoretical predictions reported in Ref. [14]. Validation shows very good agreement for decarburization in both high-carbon (C > 0.3%) and low-carbon regimes, as well as accurate prediction of the overall FeO increase in the slag. Although the model overpredicts the initial FeO production rate, it produces correct FeO levels by the end of refining.

The baseline case also demonstrates the strong time and space nature of the refining process. During the first two minutes, decarburization is rapid, and slag FeO increases slowly. Oxidation reactions occur primarily near the injection locations and are transported toward the furnace center by gas-driven stirring. During the last 10 minutes, FeO content in the slag rises significantly as carbon reactions diminish due to the low carbon concentration in the bath. The validated CFD model was then used to evaluate two additional scenarios in which oxygen injection was reduced by shutting down coherent jets. In the first case, coherent jets 1 and 3 were turned off at 200 sec; in the second, both jets #1 and #3 were turned off at 400 sec. Decarburization rates and FeO generation were compared with the baseline case, yielding the following results:

- turning off jets 1&3 at 200 sec while keeping the remaining jets active reduced decarburization performance by 5.5% and lowered FeO generation by 53.6%;
- turning off the same 1&3 jets at a later time, 400 sec, reduced impact on decarburization, 2.1% less, and led to a 41.5% reduction in FeO generation.

The impact on decarburization and FeO production was followed up by computing the slag height during the process for the baseline case and the case where jets 1 and 3 were turned off at 200 sec. These results show that it is possible to predict a relationship between oxygen use and carbon injection which could be used to optimize

the refining cycle for operational cost, productivity and emissions reduction. Future work might include taking into consideration the impact of carbon and oxygen lance practice and slag composition and temperature in respect to overall slag foaming and furnace operation. These results, along with additional scenarios simulated using the CFD platform, can be used to optimize the refining stage. While the influence of oxygen injections on refining performance observed in this study is expected to be representative of industrial EAF operations in general, the quantitative optimization trends are likely to be furnace-specific. Factors such as furnace size, coherent-jet and lance configuration, operating practices, and the target slag and molten bath conditions can significantly influence the optimal oxygen injection strategy and the resulting refining performance.

ACKNOWLEDGMENTS

The authors thank the members of the Steel Manufacturing Simulation and Visualization Consortium (SMSVC) for their support and consultation on this research. In addition, the authors would like to thank the staff and students at Purdue University Northwest's Center for Innovation through Visualization and Simulation (CIVS) for their support and for providing the resources necessary to conduct this research. This work was supported by the U.S. Department of Energy's Office of Critical Minerals and Energy Innovation under the Industrial Technologies Office (ITO) Award Number DE-EE0011212. The views expressed herein do not necessarily represent the views of the U.S. Department of Energy or the United States Government.

REFERENCES

[1] M. Fan, Z., Friedmann, S. J. (2021). Low-carbon production of iron and steel: Technology options, economic assessment, and policy. Joule, 5(4), 829-862.
[2] Banks, R. B., & Chandrasekhara, D. V. (1963). Experimental investigation of the penetration of a high-velocity gas jet through a liquid surface. Journal of Fluid Mechanics, 15(1), 13-34.
[3] Alam, M., Irons, G., Brooks, G., Fontana, A., & Naser, J. (2011). Inclined jetting and splashing in electric arc furnace steelmaking. ISIJ international, 51(9), 1439-1447.
[4] Mathur, P. C., Mahoney, W. J., Warty, S. K. and von Schéele, J. (2021). CoJet® - 25 Years of Revolutionizing EAF Steelmaking. Steel Tech Vol. 15, No 4
[5] Strelbisky, A., Strelbisky, M., & Kurisu, K. (2024). Decarbonization at Nucor Seattle using Tallman Supersonic Carbon Injectors (TSCi). In 13th European electric steelmaking conference. Stahlinstitut VDeh, Essen.
[6] Maiolo, J., Hirmiz, R., & Bielec, B. (2025). 3-in-1 Injector for EAF: Development, Laboratory Testing and Industrial Trials. In 2025 Iron and Steel Technology Conference, AISTech 2025 (pp. 635-644). Association for Iron and Steel Technology.
[7] Memoli, F., Mapelli, C., Ravanelli, P., & Corbella, M. (2004). Simulation of oxygen penetration and decarburization in EAF using supersonic injection system. ISIJ international, 44(8), 1342-1349.
[8] Wei, J. H., & Zhu, D. P. (2002). Mathematical modeling of the argon-oxygen decarburization refining process of stainless steel: Part II. Application of the model to industrial practice. Metallurgical and materials transactions B, 33(1), 121-127.
[9] Chen, Y., Silaen, A. K., & Zhou, C. Q. (2020). 3D integrated modeling of supersonic coherent jet penetration and decarburization in EAF refining process. Processes, 8(6), 700.
[10] Chen, Y., Wang, Y., Tang, G., Silaen, A. K., Vanover, K., & Zhou, C. Q. (2019). Numerical investigation of decarburization reaction characteristics in electric arc furnace steelmaking process. Association for Iron & Steel Technology. AISTech 2019 Proceedings, 789-796.
[11] Tang, G., Chen, Y., Silaen, A. K., Krotov, Y., Riley, M. F., & Zhou, C. Q. (2019). Investigation on coherent jet potential core length in an electric arc furnace. Steel Research International, 90(4), 1800381.
[12] Ugarte, O., Busa, N., Konar, B., Okosun, T., & Zhou, C. Q. (2024). Impact of Injection Rate on Flow Mixing during the Refining Stage in an Electric Arc Furnace. Metals, 14(2), 134.
[13] Kottapalli, S., Ugarte, O., Konar, B., Okosun, T., & Zhou, C. Q. (2025). CFD Modelling of Refining Behavior in EAF: Influence of Burner Arrangement and Oxygen Flow Rates. Metals, 15(7).
[14] Pretorius, E., Oltmann, H., & Jones, J. (2010). EAF fundamentals. LWB Refractories, Hilden, 14.
[15] Luo, Q., Chen, Y., Abraham, S., Wang, Y., Petty, R., Silaen, A. K., & Zhou, C. (2022). Effects of EAF operations on water- cooling panel overheating. steel research international, 93(9), 2100844.

[16] Krieger, I. M., & Dougherty, T. J. (1959). A mechanism for non-Newtonian flow in suspensions of rigid spheres. Transactions of the Society of Rheology, 3(1), 137-152.

[17] Demus, T., Echterhof, T., Pfeifer, H., Schulten, M., Noel, Y., & Quicker, P. (2012, September). Investigations on the use of biogenic residues as a substitute for fossil coal in the EAF steelmaking process. In Proceedings of the 10th European Electric Steelmaking Conference, Graz, Austria (pp. 25-28).

TORNA ALL'INDICE >